

## Readsorption and diffusion-limited TPD of water from zeolite Linde 4A

A. Palermo<sup>1</sup>, C.M. Aldao<sup>\*</sup>

*Institute of Materials Science and Technology (INTEMA), Universidad Nacional de Mar del Plata – CONICET,  
Juan B. Justo 4302, 7600 Mar del Plata, Argentina*

Received 24 February 1998; accepted 2 June 1998

---

### Abstract

Coupled effects due to diffusion and readsorption of desorbed species on temperature-programmed desorption (TPD) data have been analyzed and compared with experimental curves during TPD of water from zeolite Linde 4A. The effects of different heating rates and carrier-gas flow are considered explicitly. A simple model is presented which allows straightforward extraction of kinetic parameters from the experimental data, even in the presence of effects due to readsorption and diffusion. In this system, it is found that an extensive readsorption of gas occurs within the zeolite pellet and the local adsorbate coverage is governed by equilibrium adsorption. We found that neglecting the effects of diffusion can cause activation energy falsifications of the order of 10%. When readsorption and diffusion are not taken into account, calculated pre-exponential factors are very small and convey no direct physical meaning. © 1998 Elsevier Science B.V.

*Keywords:* Desorption; Temperature-programmed desorption; Type 4A; Zeolites

---

### 1. Introduction

Temperature-programmed desorption (TPD) is an experimental kinetic technique which allows identification of different bonding sites and evaluation of the kinetic parameters associated with those sites. Originally developed for working with single crystals, TPD studies have been extended to desorption from porous solids [1–5]. In the latter case, interpretation of the TPD data is often complicated, because the shape of the TPD spectra can be affected by diffusional resistance, readsorption, and flow rate of the carrier gas [6].

Usually, lag times in the sample cell and pore can be made negligible with a suitable design of the experiment. However, mass transport effects in porous solids could lead to concentration gradients in the sample and/or pressure build-ups that may distort the TPD results. The problem has been analyzed by Gorte [5], who proposes dimensionless groups of parameters, allowing a-priori determination of the limit values that may be used in order to obtain reliable TPD data.

Contrary to the difficulties mentioned above, readsorption is intrinsic to porous materials and often cannot be eliminated. Moreover, readsorption effects can lead to a fundamental change in the information content of the TPD spectrum. The desorption step may no longer be the rate-limiting process and the measured flux of molecules leaving the sample are instead determined by the rate of diffusion of molecules out of

---

<sup>\*</sup>Corresponding author. Tel. +54 23 810046; fax: +54 23 816600.

<sup>1</sup>Present address: Department of Chemistry, University of Cambridge, Cambridge CB2 1EW, England.

the sample pores (as modified by adsorption on the pore walls).

Cvetanovic and Amenomiya [2] have suggested that the role of readsorption can be determined by varying the flow rate of the carrier gas. Indeed, concentration gradients in the sample are controlled by the ratio of carrier-gas flow rate to diffusivity. However, this procedure is experimentally difficult in many cases and Gorte [5] has demonstrated that flow rate variations might be not informative. At low flow rates, the accumulation of gas in the sample cell controls the TPD spectra, with no significant concentration gradients in the sample, and the adsorption–desorption equilibrium is usually reached. In this low-flow-rate limit, the temperature peak is a function of the carrier-gas flow rate. For large flow rates, on the other hand, the concentration varies significantly over the width of the sample. It is not possible to assume that sufficiently high flow rates (when a further increase in the carrier-gas flow rate does not affect the TPD spectra) prevent readsorption from occurring, because flow out will be limited in the sample.

In the following sections, we outline a model for quantitative analysis of TPD spectra when readsorption is present. The simple model described below may be successfully applied to the desorption of water from zeolite Linde 4A. For highly porous solids, as zeolites, adsorption can compete with desorption during TPD experiments to the extent that adsorption equilibrium is closely approached. At or near ambient temperatures, the equilibrium isotherm is highly favorable and intracrystalline diffusion is assumed to be sufficiently rapid to maintain the sorbate concentration, essentially uniform through an individual crystallite and at equilibrium with the sorbate concentration in the macropore [7].

We will also investigate, experimentally and theoretically, the effect of heating rate and carrier-gas flow rate on TPD spectra. As the flow rates decrease, the readsorption process is found to increase. However, it is shown, for our experimental system, that the activation energy for desorption can, nevertheless, be determined by the method described by Cvetanovic and Amenomiya, independently of readsorption. For high sufficiently flow rates, TPD spectra are no longer affected, indicating that the measured flux of molecules is determined by the rate at which molecules can leave the sample.

## 2. Readsorption model without diffusion resistance

In this section, a simple analytical approach for desorption of water from zeolite type A is discussed by following the method developed by Cvetanovic and Amenomiya [2]. Lag times due to detector and thermocouple responses will be neglected since they have been shown to be easily avoidable [8–10]. In general, readsorption introduces important modifications in the shape of desorption curves, such as broadening the peaks, shifting them to higher temperatures, and smoothing out peaks corresponding to sites with higher adsorption energies [5,6,11,12]. Readsorption can be important even for high carrier-gas flow rates and also when the experiment takes place in vacuum. Also, it is important to note that the evaluation of the sticking coefficient,  $s$ , may sometimes be difficult [13].

We assume that the gas phase in the sample cell is well mixed, having a constant concentration  $c$ . When readsorption is possible, we can write the following conservation equations for the TPD system

$$-\frac{d\theta}{dt} = k_d\theta - k_a c(1 - \theta) \quad (1)$$

$$Fc = n_0[k_d\theta - k_a c(1 - \theta)] \quad (2)$$

Note that, in the above equations, we have neglected the accumulation of gas in the sample which would be represented by term  $Vdc/dt$ , because the well-mixed void volume is considered to be very small. (See Appendix A for nomenclature.)

The net desorption rate from the surface is given by

$$-\frac{d\theta}{dT} = \frac{k_d\theta}{\beta[1 + k_a\alpha(1 - \theta)]} \quad (3)$$

provided  $T$  varies according to a linear heating schedule  $T=T_0+\beta t$ ,  $\beta$  being the heating rate ( $\beta=dT/dt$ ). In Eq. (3)  $\theta=n/n_0$  ( $n_0$  is the number of available sites and  $n$  the number of adsorbed particles),  $\alpha=n_0/F$  ( $F$  is the gas flow rate), and  $k_d$  ( $k_d=A_d \exp(-E_d/RT)$ ) and  $k_a$  ( $k_a=A_{cT}vs/n_0$ ) the desorption and adsorption rates, respectively.

For  $k_a\alpha \ll 1$ , readsorption can be neglected and desorption kinetics only determines the TPD curve profile. For a first-order desorption, a plot of  $\ln(T_m^2/\beta)$  vs.  $1/T_m$  gives a straight line with a slope and intercept

equal to  $E_d/R$  and  $E_d/A_dR$ , respectively, allowing one to obtain the actual values of  $E_d$  and  $A_d$ .

In the other extreme situation, when  $k_a \alpha \gg 1$ , re-adsorption is dominant and the TPD curve profile is determined by the displacement of the adsorption/desorption equilibrium, as the temperature increases. In this case, the heating rate and position of the maximum ( $T_m$ ) are related by

$$\ln\left(\frac{T_m^2}{\beta}\right) = \ln\left(\frac{E_d \alpha (1 - \theta_m)^2 A_a}{R A_d}\right) + \frac{E_d}{RT_m} \quad (4)$$

where the expression  $(1 - \theta_m)^2$  affects the logarithm of the ordinate, at most, by a factor of  $\approx 0.25$ , since, for  $\theta_0=1$ , the coverage corresponding to the maximum is ca. 0.5. Consequently, in case when  $k_a \alpha \gg 1$ , if re-adsorption is neglected and experimental data are analyzed by plotting  $\ln(T_m^2/\beta)$  vs.  $1/T_m$ , the value of  $E_d$  can still be obtained from the slope of the straight line. However, the intercept will give an *apparent* pre-exponential factor,  $A'_d = A_d/\alpha(1 - \theta_m)^2$ : this will be too small and dependent on flow rate, as Eq. (4) qualitatively predicts.

The simple model described above can be successfully applied to the desorption of water from zeolite 4A. Under equilibrium conditions in ambient air, both, 4A and 5A zeolite samples contained ca. 18 wt.% of water. The experimental apparatus used for obtaining the TPD spectra, consisting of an electrobalance (Cahn 2000) and a temperature-programmable process controller (Omega CN3002), has been described previously [14,15]. In what follows, the observed effects of varying carrier-gas flow rates and heating rates are analyzed and discussed. It will be shown that, for real spectra data, the apparent pre-exponential factor does indeed decrease as the carrier-gas flow decreases, in accordance with theoretical predictions. This may be interpreted as an increasing possibility of re-adsorption of the molecules of water as they leave the zeolite sample.

Fig. 1 shows the experimental TPD spectra for the desorption of water from pelletized zeolite Linde 4A for different heating rates and at a constant carrier-gas flow rate,  $Q$ , for which the peak temperature is not a function of  $Q$ . These show the expected increase of  $T_m$  with the heating rates  $\beta$ . These spectra were used to construct the plot shown in Fig. 2 (●). Fig. 2 also shows similar plots obtained using different carrier-

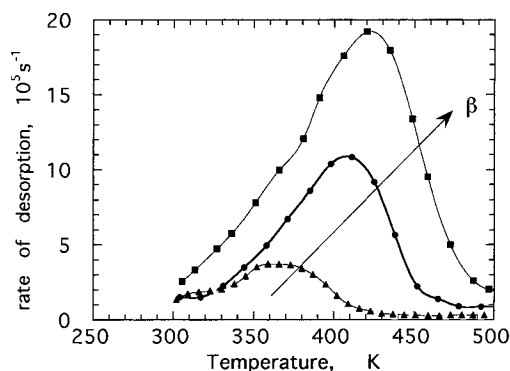


Fig. 1. Experimental TPD spectra for water desorption from pelletized Linde 4A at different heating rates and 'infinite' carrier-gas flow rate ( $\beta=0.0137, 0.018$  and  $0.057 \text{ K s}^{-1}$ ).

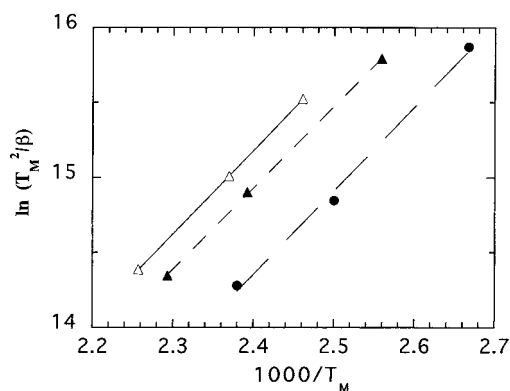


Fig. 2. Plot of  $\ln T_m^2/\beta$  vs.  $1000/T_m$  for the experimental data points of water desorption from pelletized Linde 4A. ( $\Delta$ ) denote data for very low carrier flow rates, ( $\blacktriangle$ ) denote data for intermediate  $Q$ , and the ( $\bullet$ ) represents data from Fig. 1 at 'infinite'  $Q$ . The slope of the straight lines gives  $E_d/R \sim 5540 \text{ K}$ . Determined pre-exponential factors are 1950, 1300 and  $844 \text{ s}^{-1}$ .

gas flow rates in the same range of heating rates ( $428$  and  $49 \text{ K h}^{-1}$ ) analyzed in Fig. 1 ( $\Delta$  and  $\blacktriangle$ ).

When re-adsorption is not taken into account, and as the gas-flow rate decreases, the derived pre-exponential factor for desorption decreases, but the derived activation energy does not vary. Fig. 2 also depicts the effect of the carrier-gas flow rate on the derived value for the pre-exponential factor assuming no re-adsorption is present. As  $Q$  decreases, the apparent pre-exponential calculated using this method are 1950, 1300 and  $844 \text{ s}^{-1}$ . If adsorption is not an activated process, the heat of adsorption ( $\Delta H$ ) constitutes the activation energy for desorption,  $E_d$ . In this case,

measuring  $T_m$  as a function of  $\beta$  will allow us to determine the activation energy for desorption, but the pre-exponential factor cannot be assumed to have a direct physical meaning. For sufficiently high flow rates, the shapes of the TPD spectra and  $T_m$  become independent of further increases in the carrier-gas flow rate. Thus, for our experimental data, we find that a plot of  $\ln(\beta/T_m^2)$  vs.  $1/T_m$ , (as proposed by Cvetanovic and Amenomiya [2]) can be used to determine the heat of adsorption *even though readsorption is important*. We see, however, that the effect of readsorption strongly reduces the calculated effective pre-exponential factor.

### 3. Readsorption–diffusion model

Following other authors [5], we model the TPD process as a gas-phase diffusion of desorbed species from a uniform spherical pellet of radius  $R_p$  with macroporosity  $\epsilon$  and effective diffusivity  $D$ . The pellet empties into an external volume that is well-mixed and evacuated at a constant volumetric flow rate. At the initial temperature,  $T_0$ , all adsorbate molecules are bound on the pore wall. As the temperature is increased, molecules desorb, diffuse out of the pore while undergoing occasional readsorption and, finally, are pumped out of the external volume.

For a spherical pellet, we can write the differential mole balance on the gas and surface concentrations,  $c$  and  $n$ , giving the following equations

$$\frac{\partial c}{\partial t} = D \left( \frac{\partial^2 c}{\partial r^2} + \frac{2}{r} \frac{\partial c}{\partial r} \right) - \frac{1}{V_p \epsilon} [k_a c n_0 (1 - \theta) - k_d n] \quad (5)$$

$$\frac{\partial n}{\partial t} = k_a c n_0 (1 - \theta) - k_d n \quad (6)$$

The adsorption rate,  $k_a(1-\theta)$  is considered to be independent of temperature and proportional to  $(1-\theta)$ . Other parameters are defined in the Appendix.

Macropore diffusivity,  $D$ , is calculated through

$$\frac{1}{D} = \sigma \left( \frac{1}{D_K} + \frac{1}{D_M} \right) \quad (7)$$

where  $\sigma$  represents the tortuosity factor,  $D_K$  is the Knudsen diffusivity and  $D_M$  the molecular diffusivity.

$\sigma$  takes into account that the pore diffusivity based on the pore cross-sectional area is smaller than the diffusivity in a straight cylindrical pore as a result of the two following effects: the random orientation of the pores (which gives a longer diffusion path and a reduced concentration gradient in the direction of flow) and the variation in the pore diameter. Since the tortuosity factor is essentially a geometrical factor, it should be independent of either temperature or nature of the diffusing species. A value of five for the tortuosity factor is generally accepted for zeolite type A [16]. Taking into account the effect of temperature, the diffusivity takes the form

$$D = D_0 \sqrt{\frac{T}{T_0}} \quad (8)$$

Assuming a linear adsorption isotherm, i.e. at low converges, we can write

$$n = Kc \quad (9)$$

where the adsorption equilibrium constant, and  $K$  is assumed to have the form

$$K = n_0 \frac{k_a}{k_d} \quad (10)$$

Provided that local equilibrium exists between gas-phase and adsorbed species, Eq. (9) can be substituted in Eq. (5) to eliminate  $c$ . We now introduce the dimensionless parameters

$$\eta = r/R_p$$

$$\theta = n/n_0$$

and the mass-balance equation can be written as

$$\frac{\partial}{\partial t} \left( \frac{\gamma K}{D} \right) \theta = \frac{1}{R_p^2} \left[ \frac{\partial^2 \theta}{\partial \eta^2} + \frac{2}{\eta} \frac{\partial \theta}{\partial \eta} \right] \quad (11)$$

where  $\gamma$  is defined as  $1/K + (1/V_p \epsilon) \sim 1/V_p \epsilon$ . Since  $K$  is assumed to be independent of  $\theta$  and  $\eta$  for a linear isotherm, the equation can finally be written in the following dimensionless form

$$\frac{\partial \theta}{\partial \tau} = \frac{\partial^2 \theta}{\partial \eta^2} + \frac{2}{\eta} \frac{\partial \theta}{\partial \eta} \quad (12)$$

We now follow the approach, developed by Jones and Griffin [17], incorporating all of the system-specific parameters into a dimensionless time variable

$\tau$ . This ‘pseudo time’ variable is differentially related to real time by

$$d\tau = \frac{D_0 \sqrt{T/T_0}}{\gamma R_p^2 n_0 (k_a/k_d)} dt \quad (13)$$

In solving Eq. (12), the following boundary and initial conditions must be satisfied

$$\theta = \theta_0 \quad \text{at } t = 0 \quad (14)$$

$$\theta = 0 \quad \eta = 1 \quad (15)$$

$$\frac{\partial \theta}{\partial \eta} = 0 \quad \eta = 0 \quad (16)$$

Eq. (11) can be analytically solved by the method of variable separation, i.e.

$$\theta(\eta, \tau) = \phi(\tau) \theta(\eta) \quad (17)$$

and then

$$\frac{d^2 \theta(\eta)}{d\eta^2} + \frac{2}{\eta} \frac{d\theta(\eta)}{d\eta} = -a_m^2 \theta(\eta) \quad (18)$$

$$\frac{1}{\phi(\tau)} \frac{d\phi(\tau)}{d\tau} = -a_m^2 \quad (19)$$

Joes and Griffin used dimensional analysis to obtain an expression for the concentration profile in the case of a cylindrical particle. Here, we use a different approach, involving Fourier analysis, to derive the concentration profile within a spherical particle. To solve Eq. (18), we expanded  $\theta(\eta)$  in a Fourier series. The solution for Eq. (12) is readily obtained by the change of variable  $u = \theta r$ , subject to the conditions of Eqs. (14)–(16).

Finally,  $\theta(\eta, \tau)$  can be written as

$$\frac{\theta(\eta, \tau)}{\theta_0} = \frac{-2}{\pi} \sum_n \phi(\tau) \frac{(-1)^n}{n} \sin(n\pi\eta) \quad (20)$$

By solving the above equation, the concentration profiles within the pellet at successive stages of desorption can be determined, as shown in Fig. 3. Note that these profiles are completely general for all adsorbates exhibiting a linear (Henry) isotherm. Fig. 4 shows the amount of adsorbate remaining in the pellet as a function of the dimensionless time variable,  $\tau$ .

The desorption rate at a real time over the entire surface,  $r_d$ , can be obtained as follows

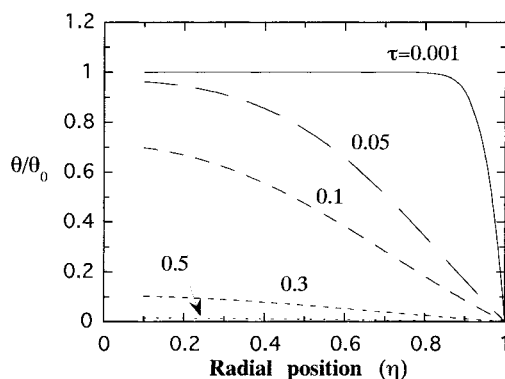


Fig. 3. Concentrations profiles within the sample at successive stages of development for a linear adsorption isotherm.

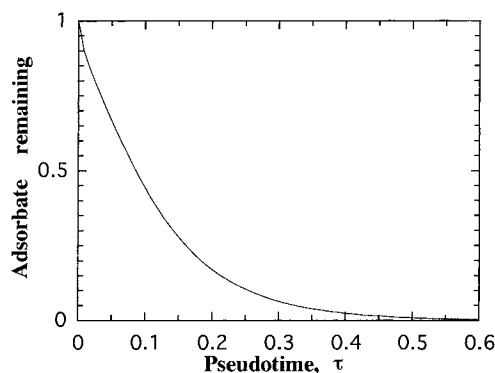


Fig. 4. Amount of adsorbate remaining in the sample as a function of the pseudo time.

$$r_d = -A \left( D_0 \sqrt{T/T_0} \frac{\partial c}{\partial r} \right) \Big|_{r=R_p} \quad (21)$$

The desorbing flux is calculated as a function of  $\tau$  and then related with the real time by integrating Eq. (13), as discussed below.

For the readsorption–diffusion model, the desorption process can best be thought of as a diffusional emptying of a finite porous medium, modified by readsorption of the diffusing species. The peak in the TPD spectrum arises from the highly non-linear temperature dependence of the adsorption equilibrium constant. At low temperatures, transport out of the sample occurs slowly because molecules spend most of their time in the adsorbed state. As the temperature is increased, molecules spend more time in the gas

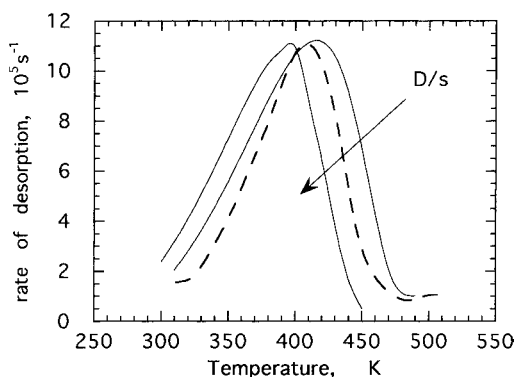


Fig. 5. Calculated TPD spectra for  $D/s=5.10^{-6}$  and  $5.10^{-5} \text{ m}^2 \text{ s}^{-1}$ . Dashed curve represents the experimental spectrum. Note that, with  $E_d/R \sim 5540 \text{ K}$ , it is not possible to find the data.

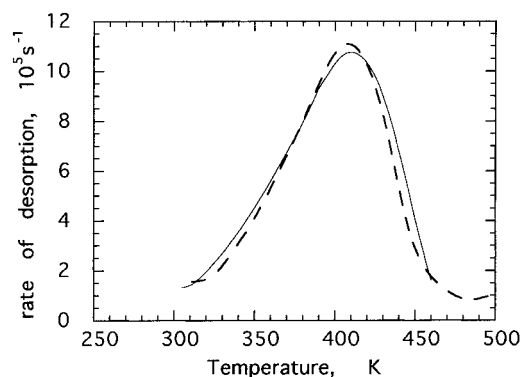


Fig. 6. Calculated TPD spectra with  $E_d/R=6500 \text{ K}$  and  $D/s=5.10^{-6} \text{ m}^2 \text{ s}^{-1}$ . Dashed curve represents the experimental spectrum.

phase, and diffusion out of the sample occurs at an increasing rate. Although, the molecules leave the sample due to diffusion the total flux is essentially controlled by desorption. If, for any reason, desorbed molecules cannot leave the pellet, the concentration in the gas phase  $c$  will rapidly increase and then the measured desorption rate will not be greatly affected. Hence, in contrast to what one might expect, our TPD curves *do not strongly depend* on the exact value of diffusivity as will be shown below.

Fig. 5 shows the TPD spectra for water desorption from zeolite 4A at a constant heating rate of  $0.018 \text{ K s}^{-1}$ . The dashed curve in this figure represents, the experimental TPD spectrum for water desorption from commercial zeolite pellets Linde 4A. Fig. 5 also depicts two calculated TPD spectra corresponding to the readsorption–diffusion model, which illustrate the effects of diffusivity and sticking coefficient. Note that spectra scale with the ratio diffusivity/sticking coefficient. We assume a ‘normal’ value for the pre-exponential factor for desorption, namely  $10^{-13} \text{ s}^{-1}$ . As can be seen, simulated curves, using the previously determined value of the activation energy ( $E_d/R=5540 \text{ K}$ ) obtained using the simple model, are wider than the experimental one. If we take the activation energy,  $E_d$ , as a fitting parameter, as shown in Fig. 6, the theoretical curve matches the experimental one with an activation energy greater than before ( $E_d/R=6500 \text{ K}$ ) and with a  $D/s$  value of ca.  $5.10^{-6} \text{ m}^2 \text{ s}^{-1}$ . If  $D$  is of the order of  $5.10^{-7} \text{ m}^2 \text{ s}^{-1}$ , we can estimate  $s$  to be of the order of 0.1.

Table 1

Kinetic parameters for water desorption from Linde 5A zeolite

Desorption peak	$A'_d$ ( $\text{s}^{-1}$ ) [14]	$A_d$ ( $\text{s}^{-1}$ ) this work	$E_d/R$ (K) this work
I	539	$10^{13}$	4200
II	3747	$10^{13}$	5700
III	459142	$10^{13}$	8500

The analysis presented here can be extended to water desorption from zeolite Linde 5A as this system shows the same behavior as the water–zeolite 4A case, but with three binding states for adsorption [14], as it can be seen from Table 1. In our earlier work, the kinetic parameters for the desorption of water from zeolite 5A at maximum coverage were reported. From the kinetic parameters listed in Table 1, it appears that a compensation effect exists, i.e. there is a linear relationship between the logarithm of the pre-exponential factor and the activation energy [14,18]. The linearity between  $\ln A$  and  $E_d$  suggests the existence of an isokinetic characteristic temperature at which all rates are equal. We have re-examined this data, using the readsorption–diffusion model described above, in the light of our conclusions. As it can be seen from Table 1, we were able to fit the whole set of experimental curves with a unique constant pre-exponential factor. In this connection, we conclude that this *apparent* compensation effect previously reported is, in fact, just an artifact resulting from falsification

of kinetic parameters due to the effects of readsorption and diffusion.

#### 4. Conclusions

A model to describe the thermal desorption process from porous samples with readsorption has been formulated and applied to water desorption from zeolite Linde 4A. The effects of different heating rates and carrier-gas flow have been investigated experimentally and the results analyzed in terms of our simple model which allows straightforward extraction of kinetic parameters from the experimental data, even in the presence of effects due to readsorption and diffusion. In this system, it is found that gas readsorption occurs extensively within the zeolite pellet and that the local adsorbate coverage is in adsorption equilibrium. Reasonably accurate estimates of adsorption energies can be obtained using a simple model based on the assumption of equilibrium adsorption, in the absence of gradients in the adsorbate concentration. The use of this model to determine the pre-exponential factor for desorption produces large errors when significant readsorption is present and the pre-exponential factor is too small and dependent on carrier-gas flow rate.

When the effects of diffusion and readsorption in the pellet are taken into account (readsorption–diffusion model), we obtained an expression for the concentration profile in a spherical particle, solving the relevant equation by a much simpler method than that used by other authors who have examined the related case for a cylindrical particle. We showed that neglecting the effects of diffusion can cause activation energy falsification of the order of 10%, compared with the values obtained when diffusion is not taken into account (readsorption without diffusion resistance model). We also showed that neglecting readsorption and diffusion results in calculated pre-exponential factors that are very small and convey no direct physical meaning.

#### Acknowledgements

This work was supported by the National Council for Scientific and Technical Research of Argentina (CONICET) and the University of Mar del Plata.

## Appendix A

### Nomenclature

$A$	external surface area ( $\text{m}^2$ )
$A_{cT}$	total area
$A_a$	pre-exponential factor for adsorption ( $\text{s}^{-1}$ )
$A_d$	pre-exponential factor for desorption ( $\text{s}^{-1}$ )
$c$	gas-phase concentration (molecules/ $\text{m}^3$ )
$D, k_a, D_m, D_0$	effective diffusivity, Knudsen, molecular and effective diffusivity for $T=T_0$ ( $\text{m}^2/\text{s}$ ) ( $\text{m}^2/\text{s}$ )
$E_a$	activation energy for adsorption
$E_d$	activation energy for desorption
$F$	flow rate of gas ( $\text{m}^3/\text{s}$ )
$k_a$	adsorption rate constant, $k_a=A_{cT}v_s/n_0$ ( $\text{m}^3\text{s}^{-1}$ )
$k_d$	desorption rate constant, $k_d=A_d \exp(-E_d/RT)$ ( $\text{s}^{-1}$ )
$K$	equilibrium constant for adsorption ( $\text{m}^3$ )
$M$	molecular weight
$n, n_0$	number of adsorbed particles, number of available sites
$\Delta H=(E_a-E_d)$	heat of adsorption
$Q$	flow rate of the carrier gas ( $\text{m}^3/\text{s}$ )
$r_a, r_d$	adsorption and desorption rate (molecules/s)
$R$	gas constant
$R_p$	radius of pellet (m)
$t$	time (s)
$T, t_0, T_m$	temperature, initial and at peak maximum (K)
$s$	sticking coefficient
$v$	velocity of gas to the surface ( $v = \sqrt{RT/2\pi M}$ ) in (m/s)
$V$	volume of the sample ( $\text{m}^3$ )
$V_p$	volume of the pellet ( $\text{m}^3$ )
$\alpha$	parameter for readsorption ( $\alpha=n_0/F$ ) ( $\text{s}/\text{m}^3$ )
$\beta$	temperature increasing rate (K/s)
$\epsilon$	macroporosity ( $\text{m}^3/\text{m}^3$ )
$\theta, \theta_0$	fraction of occupied sites at time $t$ and $t=0$
$\theta_m$	fraction of occupied sites at $T_m$
$\sigma$	tortuosity factor

**References**

- [1] P.A. Redhead, *Vacuum* 12 (1962) 203.
- [2] R.J. Cvetanovic, Y. Amenomiya, *Catal. Rev.* 6 (1972) 21.
- [3] (a) H. Froitzheim, P. Schenk, G. Wedler, *J. Vac. Sci. Technol. A* 11 (1993) 2; (b) R.M. Ormerod, R.M. Lambert, D.W. Bennet, W.T. Tysoe, *Surf. Sci.* 330 (1995) 1.
- [4] J.L. Falconer, J.A. Schwarz, *Catal. Rev.* 25 (1983) 2.
- [5] R.J. Gorte, *J. Catal.* 75 (1982) 164.
- [6] J.S. Rieck, A.T. Bell, *J. Catal.* 85 (1984) 143.
- [7] N. Wakao, S. Kaguci, N. Nagai, *Chem. Eng. Sci.* 33 (1978) 193.
- [8] R.K. Herz, J.B. Kiela, S.P. Marion, *J. Catal.* 73 (1982) 66.
- [9] R.N. Carter, B. Anton, *J. Vac. Sci. Technol. A* 10 (1992) 2.
- [10] F.E. Ibok, D.F. Ollis, *J. Catal.* 50 (1983) 391.
- [11] (a) J.A. Horas, D.A. Rodriguez Saa, G. Zgrablich, *Lat. Am. Appl. Res.* 19 (1989) 111; (b) J.L. Sales, R.O. Unac, M.V. Gargiulo, V. Bustos, G. Zgrablich, *Langmuir* 12 (1996) 95.
- [12] D. Edwards, *Surf. Sci.* 49 (1975) 393.
- [13] T. Nordmeyer, F. Zaera, *J. Chem. Phys.* 97 (1992) 9345.
- [14] A. Palermo, D.G. Löffler, *Thermoch. Acta* 159 (1990) 171.
- [15] J.R. Sánchez, A. Palermo, C.M. Aldao, *Langmuir* 12 (1996) 36.
- [16] D.M. Ruthven, *Principles of Adsorption and Adsorption Processes*, Wiley, New York, 1984.
- [17] D.M. Jones, G.L. Griffin, *J. Catal.* 80 (1983) 1.
- [18] A. Palermo, M.P. Suárez, C.M. Aldao, *Lat. Am. Appl. Res.* 24 (1994) 219.